C–C Bond as Shuttle of Two Electrons in Intermolecular and Intramolecular Processes: A Theoretical Approach to Molecular Batteries

Marzio Rosi,[a] Antonio Sgamellotti,*[a] Federico Franceschi,[b] Carlo Floriani[b]

Abstract: Density functional calculations have been carried out on titanium Schiff base complexes and titanium porphyrinogen complexes in order to understand the behavior of these systems in redox processes. In titanium Schiff base complexes C–C σ bonds are formed upon the acquisition of pairs of electrons, while in titanium porphyrinogen complexes C–C σ bonds are formed upon the donation of pairs of electrons. In both systems, the formation or the breaking of C–C bonds avoids a variation in the oxidation state of the metal. These C–C bonds, therefore, act not only as electron reservoirs, but also as a buffer for the oxidation state of the metal.

Keywords: density functional calculations · electron reservoirs · molecular batteries · porphyrinogens · Schiff bases · titanium

Introduction

The most common mechanisms by which we can store and release electrons involve coordination compounds, in which the electrons are made available through a variation in the oxidation state of the metal and polyaromatic systems, able to accept electrons in the π^* orbitals. More recently systems in which the *electron reservoir* is a C–C σ bond have been investigated.[1–5] In this context, we can distinguish between two main classes of compounds: i) transition metal Schiff base complexes, in which the C–C σ bond arises from a reductive process, as depicted in Scheme 1, and ii) porphyrinogen complexes, in which the C–C σ bond originates from an oxidative process, as shown in Scheme 2.

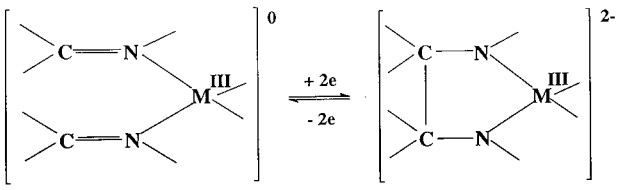

Scheme 1. C–C σ bond formation upon a reductive process.

[a] Prof. Dr. Antonio Sgamellotti, Prof. Dr. Marzio Rosi
Centro di Studi CNR per il Calcolo Intensivo in Scienze Molecolari and Dipartimento di Chimica, Università di Perugia
via Elce di Sotto 8, 06123 Perugia (Italy)
Fax: (+39) 075-5855606
E-mail: sgam@thch.unipg.it

[b] Dr. Federico Franceschi, Prof. Dr. Carlo Floriani
Institut de Chimie Minérale et Analytique
BCH Université de Lausanne, 1015, Lausanne (Switzerland)

In both classes of compounds, systems that show a redox process which is reversible have been synthesized.[1–5] Because of this peculiarity, these systems are particularly interesting for the design of molecular batteries. The first class of compounds includes systems in which the formation of the C–C bonds occurs through the reversible reductive coupling of imino groups belonging to a tetradentate Schiff base ligand, for example, salophen [*N*,*N*′-phenylenebis(salicylideneaminato) dianion] (see Figure 1) bonded to a transition metal. Complexes of titanium,[1] vanadium,[1] manganese,[2] zirconium[3] and cobalt[4] have been recently reported. The reductive coupling of imino groups is an intramolecular process in the manganese system, while it is intermolecular for the other complexes. The second class of compounds consists of metals coordinated by the *meso*-octaethylporphyrinogen tetraanion[6] (see Figure 2); these compounds have an unusual redox chemistry. Indeed, the absence of *meso*-hydrogen atoms in the *meso*-octaethylporphyrinogen prevents the aromatization to porphyrin. The complexation of several metals by *meso*-octaethylporphyrinogen has been recently reported.[5] In these complexes an oxidative process implies the formation of cyclopropane units within the porphyrinogen skeleton. The cyclopropane units can be seen as two-electron shuttles, since the redox process is reversible.[7]

The present paper is focused on density functional calculations on model systems of the above-mentioned classes of complexes; these calculations were performed in order to understand how C–C units can function as electron shuttles in redox processes, the role played by the metal, and the requisites for the reversibility of the electron storage.

$[Ti(salophen)Cl_2]$ and $[Ti(salophen)]_2^{2+}$ were considered as models of oxidized transition metal Schiff base complexes, while $[Ti_2(*salophen_2*)]^{2-}$, in which $*salophen_2*$ (see

  0947-6539/99/0510-2914 $ 17.50+.50/0

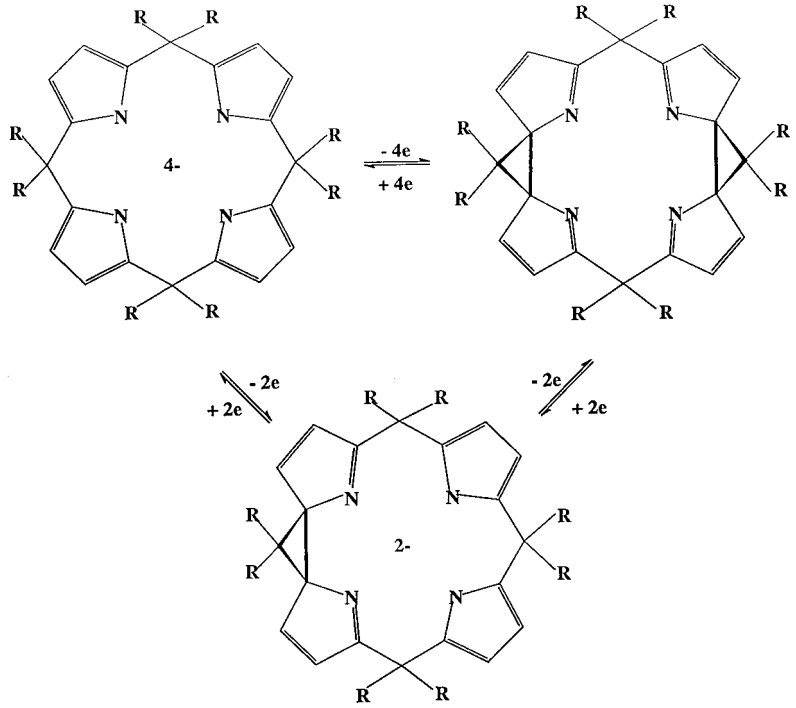

Scheme 2. C–C σ bond formation upon an oxidative process.

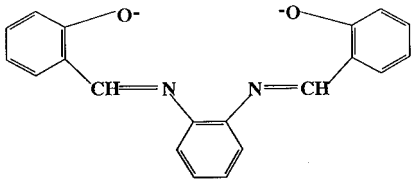

Figure 1. Salophen ligand.

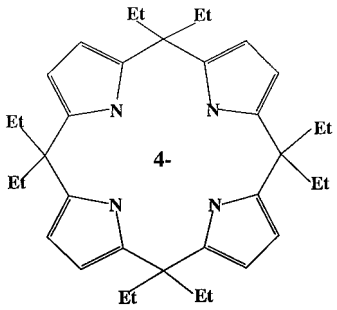

Figure 2. *meso*-Octaethylporphyrinogen tetraanion ligand.

Abstract in Italian: *Sono stati studiati mediante calcoli DFT complessi del titanio con basi di Schiff e con il porfirinogeno allo scopo di comprenderne il comportamento in processi redox. Nei complessi del titanio con basi di Schiff si ha formazione di legami σ C–C in seguito all'acquisto di coppie di elettroni, mentre nei complessi del titanio con il porfirinogeno i legami σ C–C si formano in seguito alla perdita di coppie di elettroni. In entrambi i sistemi la formazione o la rottura di legami C–C evita una variazione nello stato di ossidazione del metallo. Questi legami C–C agiscono quindi non solo da serbatoi di elettroni, ma anche da sistemi tampone per lo stato di ossidazione del metallo.*

Figure 3) functions as a dinucleating, octadentate, octaanionic ligand, was considered as a model of a reduced, iminocoupled, transition metal Schiff base complex. The latter is closely related to the experimentally characterized species $[Ti_2(*salophen_2*)(Na_2)(thf)_6]$.[1] In order to make calculations feasible, some simplifications have been made to the model representation of the salophen ligand (see below).

For the second class of complexes, porphyrinogen complexes of titanium were considered. In the experimental complexes the *meso* groups are usually ethyl groups, and it is of fundamental importance that they are different from hydrogen in order to avoid the conversion of the porphyrinogen into a porphyrin;[7] however,

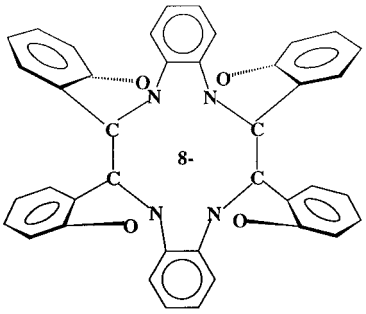

Figure 3. *Salophen$_2$* ligand.

from an electronic point of view, we do not expect to find a very different situation when the *meso* groups are ethyl groups or hydrogen atoms. For this reason we considered hydrogen instead of ethyl groups in order to simplify the calculations. Apart from this simplification, the investigated model systems are strictly related to the experimentally characterized complexes.[5]

Computational Details

Methods: Density functional theory (DFT), which has been found to be a very cost effective method to study transition metal systems,[8] was used for the determination of equilibrium geometries and the evaluation of the energetics of all the investigated systems and processes. The BP86 exchange-correlation functional was used for all the calculations. This functional is based on Becke's functional[9] and includes Slater exchange along with corrections that involve the gradient of the density for the exchange potential together with the local gradient-corrected correlation functional proposed by Perdew.[10] Open-shell systems were calculated with the spin-unrestricted approach. All the calculations were performed by using the Gaussian 94 program package[11] and were done on a cluster of

IBM RISC/6000 workstations. The atomic charges were obtained through a natural bond orbital (NBO) analysis[12] by means of the NBO program.[13]

Basis sets: The basis set employed for the calculations on the titanium Schiff base complexes was based on the Wachters–Hay set[14] for the transition metal atom and on the 6-31G* set[15] for all the other atoms, except chlorine, which was described with a 6-31G set.[15] The same basis set, with the addition of diffuse functions[16] on nitrogen, was used for most of the calculations performed on the titanium porphyrinogen complexes. Owing to the size of these systems, however, some geometric optimizations of these complexes were performed with a smaller set, based on the Wachters–Hay set[14] for the transition metal atom, the 6-31G set[15] for nitrogen and the 3-21G set[17] for carbon and hydrogen. Only the spherical harmonic components of the basis sets are used.

Model systems and geometry optimization: In order to make the calculation feasible, the salophen ligand in the transition metal Schiff base complexes was simplified by replacing the aromatic rings with C=C double bonds. This simplified ligand (see Figure 4) will be called salophen′, hereafter. The geometry of the model systems considered was fully optimized starting from parameters deduced from the available experimental X-ray structures. We considered C_{2v} symmetry for [Ti(salophen′)-Cl_2], and C_i symmetry for $[Ti(salophen')]_2^{2+}$ and $[Ti_2(*salophen'_2*)]^{2-}$.

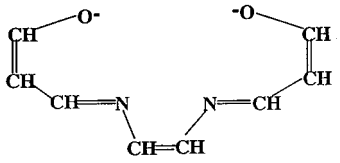

salophen'

Figure 4. Model representation of the salophen ligand.

For the metal porphyrinogen complexes, first we fully optimized the geometry of $[H_8N_4]^{4-}$ and $[H_8N_4(\Delta)_2]$, where $[H_8N_4H_4]$ is the porphyrinogen and Δ denotes a cyclopropane unit, in order to compare the reduced with the oxidized forms of the free ligand. Starting from this optimized geometry for the ligands, we subsequently optimized the geometry of the titanium complexes. We considered both the species $[H_8N_4M^{IV}]$ and $[H_8N_4(\Delta)_2M^0]$ in order to analyze the relative stability. The geometry optimizations of the free ligands were performed with the larger basis set, while those of the complexes were performed with the smaller basis set; for the titanium complexes, however, we computed the energies at the optimized geometries also with the larger basis set. The optimizations were performed considering an S_4 symmetry for $[H_8N_4M]$ and a C_2 symmetry for $[H_8N_4(\Delta)_2M]$. The fully optimized geometries of all the investigated species are available from the authors on request.

Results and Discussion

Titanium Schiff base complexes: The optimized structures of the oxidized and reduced forms of the titanium Schiff base model systems investigated are reported in Figures 5–7. Figure 5 shows the optimized structure of [Ti(salophen′)Cl_2], in which salophen′ denotes the simplified form of salophen we have considered in our model systems (see above). This structure shows an octahedral coordination around the transition metal and is similar, as expected, to that experimentally found for [Zr(salophen)Cl_2(thf)].[3] Figure 6 depicts the optimized geometry of the dimeric species $[Ti(salophen')]_2^{2+}$. The coordination around the metal is square pyramidal, since we have omitted in our model the presence of the sixth ligand (chlorine) in order to simplify the calculation. The structure is similar to the one reported for

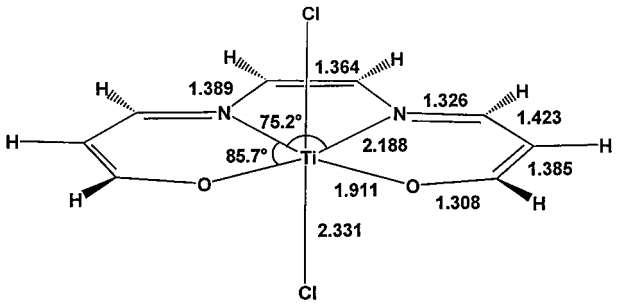

Figure 5. Optimized structure of [Ti(salophen′)Cl_2]. For clarity only the main geometrical parameters are shown. Bond lengths in Å, angles in °.

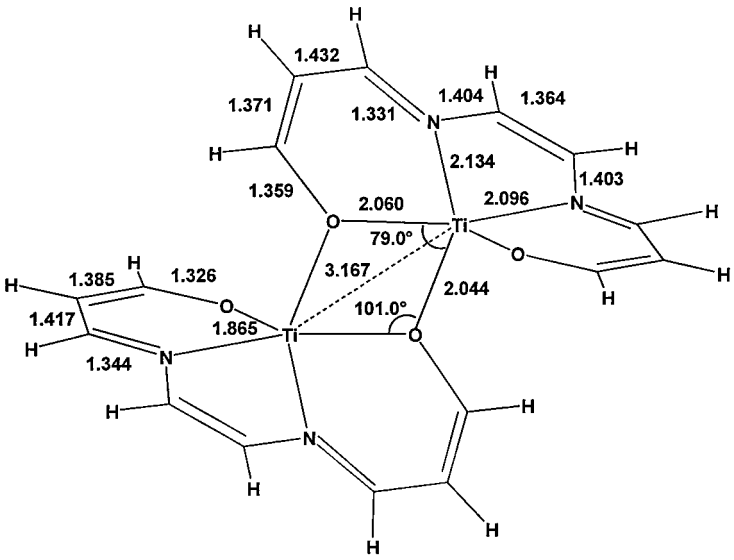

Figure 6. Optimized structure of $[Ti(salophen')]_2^{2+}$. For clarity only the main geometrical parameters are shown. Bond lengths in Å, angles in °.

[Mn(salophen)(Py)]$_2$,[2] with oxygen bridges between the two metal centers. The optimized titanium–titanium distance is computed to be 3.167 Å, and this value suggests the lack of any interaction between the two metals. Figure 7 shows the optimized geometry of $[Ti_2(*salophen'_2*)]^{2-}$. The main features of this structure are a clear rearrangement of the geometry of the salophen′ ligands, the presence of two C–C bonds (r(C–C) = 1.618 Å) between carbon atoms of imino groups of the two original salophen′ ligands, and the presence

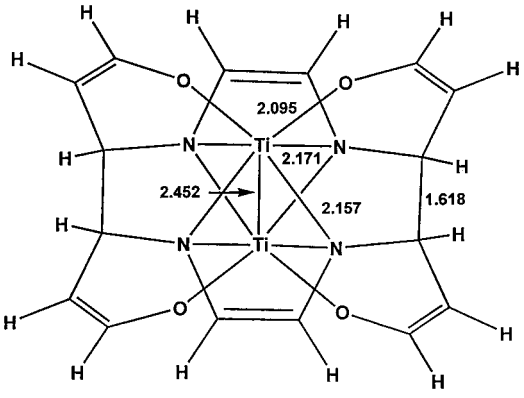

Figure 7. Optimized structure of $[Ti_2(*salophen'_2*)]^{2-}$. For clarity only the main geometrical parameters are shown. Bond lengths in Å, angles in °.

0947-6539/99/0510-2916 $ 17.50+.50/0 *Chem. Eur. J.* **1999**, *5*, No. 10

of an interaction between the two metal centers, the titanium–titanium distance being 2.452 Å. The geometry of this species can be compared directly with that found in the X-ray structure of $[Ti_2(*salophen_2*)(Na_2)(thf)_6]$:[1] our model system, indeed, only differs from the experimental system in the lack of the Na^+ cations and solvent molecules, and in the simplifications in the ligand, as mentioned above. Table 1 gives the main geometrical parameters of the model system

Table 1. Main geometrical parameters of the optimized structure of $[Ti_2(*salophen'_2*)]^{2-}$, compared with the experimental geometry of $[Ti_2(*salophen_2*)(Na_2)(thf)_6]$. Prime denotes a different salophen unit. Bond lengths in Å, angles in degrees.

Parameter	Optimized	Experimental
r(Ti–Ti′)	2.452	2.518
r(Ti–O)	2.095	2.051
r(Ti–N)	2.171	2.134
r(Ti–N′)	2.157	2.124
r(C–O)	1.310	1.330
r(N–C)	1.498	1.464
	1.395	1.398
r(C–C)	1.513	1.516
r(C–C′)	1.618	1.605
∢N′TiN′	74.5	69.6
∢NTiN′	68.3	69.7
	111.0	107.5
∢OTiN′	91.6	98.0
	146.3	157.9
∢OTiN	91.0	83.6
	144.7	132.4
∢OTiO	83.3	87.4
∢TiOC	125.0	133.2
∢TiNC	108.7	110.1
∢TiN′C′	119.5	114.8

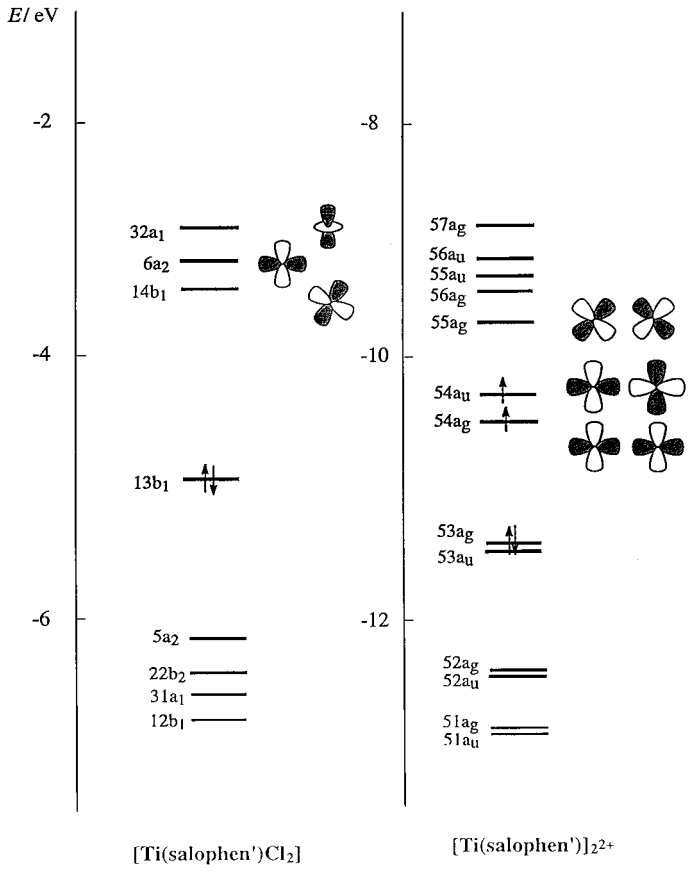

Figure 8. Frontier orbitals of the oxidized species $[Ti(salophen')Cl_2]$ and $[Ti(salophen')]_2^{2+}$.

$[Ti_2(*salophen'_2*)]^{2-}$ and the experimental species $[Ti_2(*salophen_2*)(Na_2)(thf)_6]$.[1] The agreement between the optimized and the experimental values is generally very good; this suggests that the simplifications we made in the ligand are acceptable. Significant differences are observed only for the bond angles; this is to be expected as a result of the presence in the model system of the salophen′ ligand, which is more flexible with respect to the rigid salophen ligand. We can deduce, therefore, that the main differences between the model system and the experimental complex are in the steric conformation and not in the electronic structure.

Figure 8 shows the energy levels of the frontier orbitals of the oxidized species $[Ti(salophen')Cl_2]$ and $[Ti(salophen')]_2^{2+}$. In order to simplify the description for $[Ti(salophen')]_2^{2+}$, we consider a spin-restricted picture, since the α and β orbitals are very close in energy, although the calculation was performed at a spin-unrestricted level. The ground state of $[Ti(salophen')Cl_2]$ is the singlet $^1A_1$, and the highest occupied molecular orbital (HOMO) is $13b_1$, which is mainly localized on the salophen′ ligand. The lowest unoccupied molecular orbital (LUMO) and the orbitals immediately at higher energy have mainly titanium d character, with small C=N π-antibonding components. The ground state of $[Ti(salophen')]_2^{2+}$ is the triplet ^3A_u. The $53a_u$ and $53a_g$ orbitals are doubly occupied and are mainly salophen′ in character, while the $54a_g$ and $54a_u$ are singly occupied and are essentially metal in character. In particular, these last two orbitals are the bonding and antibonding combination, respectively, of the $d_{x^2-y^2}$ orbitals of the two titanium atoms. In the complex, the Ti_2O_2 core lies on the xy plane, with the Ti atoms along the x axis. The bonding and antibonding combinations of $d_{x^2-y^2}$ are almost degenerate, since the two titanium atoms are far away (r(Ti–Ti) = 3.167 Å) and do not interact at all. For this reason these orbitals are both singly occupied. The LUMO and the orbitals immediately above are mainly bonding and antibonding combinations of d orbitals of the two titanium atoms.

In both the model systems we have considered for the oxidized species, we notice that the LUMO is mainly metal d in character. A reductive process should involve the metal, with a change in its oxidation state, at least in so far as the structure of the complex does not change.

Figure 9 depicts the frontier orbitals of the reduced species $[Ti_2(*salophen'_2*)]^{2-}$. The ground state is the singlet ^1A_g, and the HOMO is the orbital $55a_g$, which is the bonding combination of the $d_{x^2-y^2}$ orbitals of the two titanium atoms. Since the metal centers lie along the y axis we can say that there is a σ bond between the two metal centers, and this is in agreement with the relatively short Ti–Ti distance equal to 2.452 Å. The orbitals immediately lower in energy are mainly ligand (nitrogen) in character. The C–C σ bonds of the imino groups of the two different salophen units are described by the orbitals $47a_g$ and $48a_u$ which lie at even lower energy. The LUMO is a bonding combination of metal d orbitals.

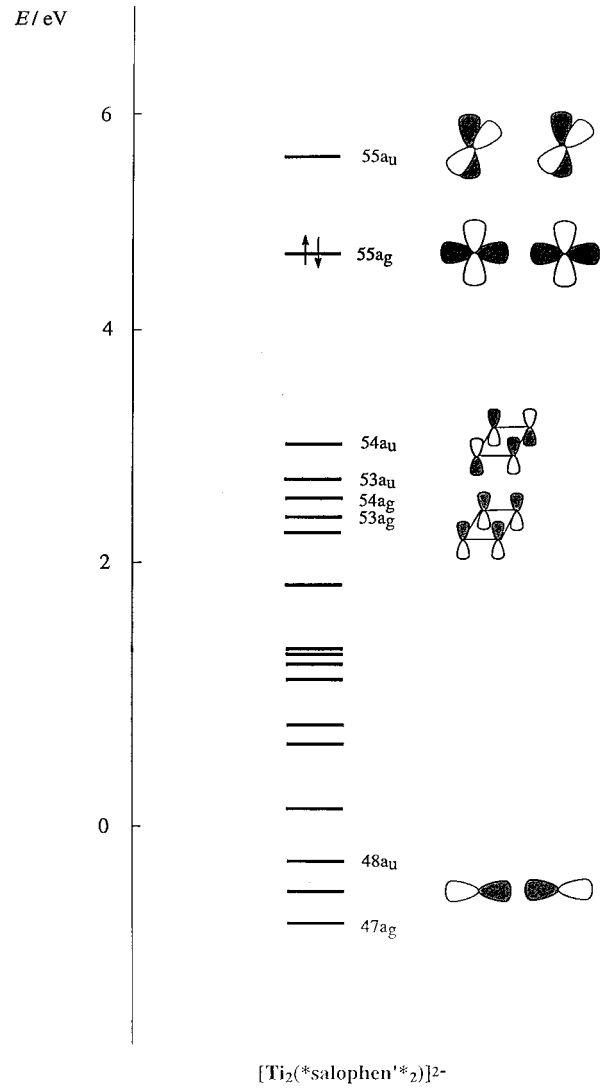

Figure 9. Frontier orbitals of the reduced species $[Ti_2(*salophen'_2*)]^{2-}$.

It is interesting to note that an oxidative process of this system involves in the first place the metal centers and should cause a change in the oxidation state of the metal. The charge on the titanium atoms, obtained through a natural bond orbital (NBO) analysis,[12] however, does not differ appreciably between the oxidized species $[Ti(salophen')]_2^{2+}$ and the reduced species $[Ti_2(*salophen'_2*)]^{2-}$: in the first system it is 1.24 e and in the latter 1.18 e. We can say at this point that in the redox process the metal is the first species that acquires or loses electrons, but the geometry rearrangement of the system is able to buffer the variation in the number of the electrons and to maintain an unchanged oxidation state of the metal.

Titanium porphyrinogen complexes: Let us start our analysis with the free ligands. The fully optimized structures of $[H_8N_4]^{4-}$ and $[H_8N_4(\Delta)_2]$ are shown in Figures 10 and 11, and their total energies are reported in Table 2. From Figure 10, we can see that $[H_8N_4]^{4-}$ has a very distorted structure that allows the nitrogen atoms, which carry most of the negative charge, to be as far away as possible from each other. From Figure 11 we can see that $[H_8N_4(\Delta)_2]$ has a calix structure, with

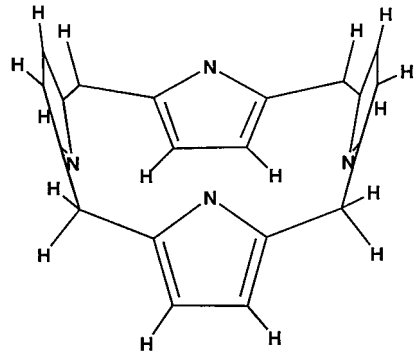

Figure 10. Optimized structure of $[H_8N_4]^{4-}$.

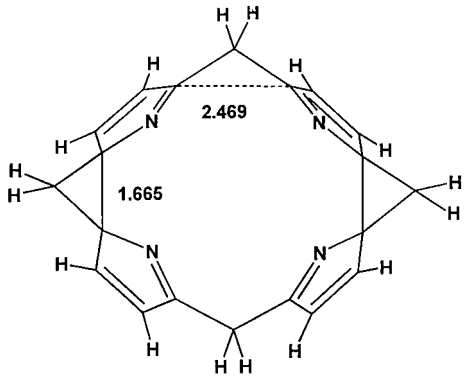

Figure 11. Optimized structure of $[H_8N_4(\Delta)_2]$. For clarity only the main geometrical parameters are shown. Bond lengths in Å, angles in °.

Table 2. Total energies (hartree) [atomic units] of the titanium porphyrinogen complexes.

	Smaller basis set	Larger basis set
$(H_8N_4)^{4-}$		– 990.175752
$(H_8N_4(\Delta)_2)$		– 990.602776
(H_8N_4Ti)	– 1836.081799	– 1840.381424
$(H_8N_4(\Delta)_2Ti)^{4+}$	– 1834.381183	
$(H_8N_4(\Delta)_2Ti)(^5A)$	– 1835.895905	– 1840.225565
$(H_8N_4(\Delta)_2Ti)(^3A)$	– 1835.880065	

the two cyclopropane rings pointing away from the cavity of the system. From the energies reported in Table 2, we can note that the reduced species is strongly destabilized, mainly because of the repulsive interactions among the negatively charged nitrogen atoms. The redox cycle shown in Scheme 2, therefore, does not seem to be possible for the free ligands.

In the next step, we considered the presence of a Ti^{4+} ion interacting with the ligands. The optimized structures of $[H_8N_4Ti]$ and $[H_8N_4(\Delta)_2Ti]^{4+}$ are shown in Figures 12 and 13, respectively. The geometry optimizations of these systems have been performed with the smaller basis set. From Figure 12 we see that the presence of the metal in the middle of the N_4 core gives rise to an almost planar structure, because of the presence of the four Ti–N bonds. From Figure 13 we can see that in $[H_8N_4(\Delta)_2Ti]$ the metal is located on top of the calix; the structure of the ligand in this case is similar to the one optimized for the metal-free species. The energies of these species are reported in Table 2 and from these values we

0947-6539/99/0510-2918 $ 17.50+.50/0 *Chem. Eur. J.* **1999**, *5*, No. 10

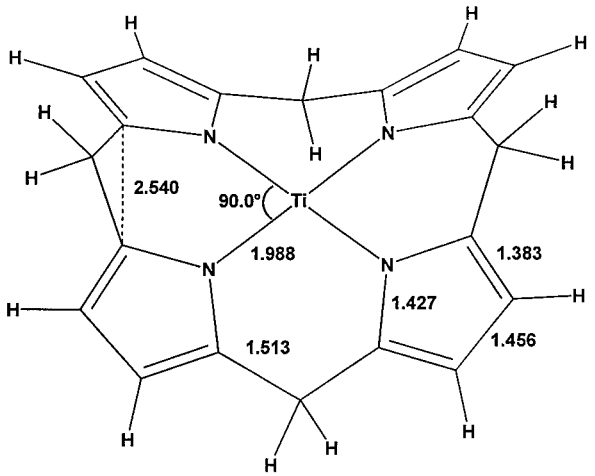

Figure 12. Optimized structure of $[H_8N_4Ti]$. For clarity only the main geometrical parameters are shown. Bond lengths in Å, angles in °.

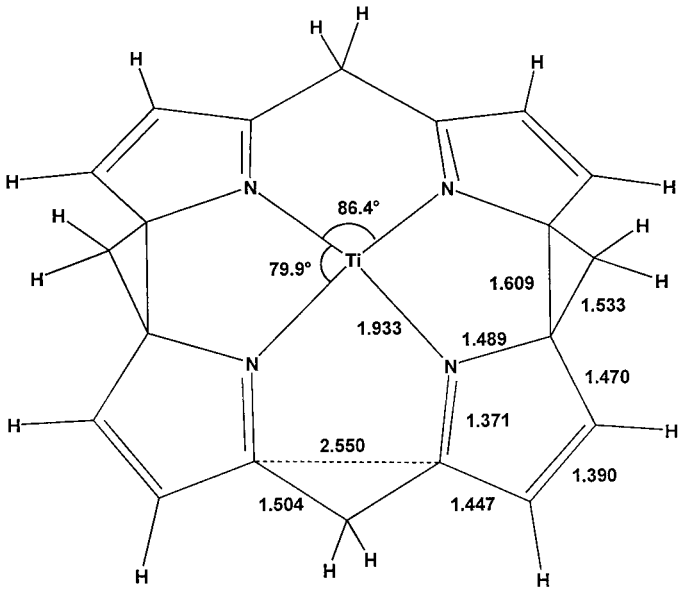

Figure 13. Optimized structure of $[H_8N_4(\Delta)_2Ti]^{4+}$. For clarity only the main geometrical parameters are shown. Bond lengths in Å, angles in °.

can see that the reduced species in this case is much more stable than the oxidized one, as expected.

In order to compare species with the same number of electrons, we also considered the system $[H_8N_4(\Delta)_2Ti^0]$. However, the geometry optimization of $[H_8N_4(\Delta)_2Ti^0]$ converges to the geometry of $[H_8N_4Ti^{IV}]$, confirming that a metal like titanium which is difficult to reduce prefers high oxidation states in the presence of a ligand able to accept electrons. The only way to study the electronic structure of $[H_8N_4(\Delta)_2Ti^0]$ was to assume a fixed geometry for this species; we considered the same geometry as that for $[H_8N_4(\Delta)_2Ti^{IV}]^{4+}$. The ground state of $[H_8N_4(\Delta)_2Ti^0]$ was computed to be a quintet, with a triplet state only 9.9 kcal mol^{-1} above. This quintet state was computed, with the larger basis set (see Table 2), to be 97.8 kcal mol^{-1} above the ground state of $[H_8N_4Ti^{IV}]$. We can conclude that titanium prefers high oxidation states in the presence of ligands like porphyrinogen that are able to accept electrons. An intramolecular redox process involving the species $[H_8N_4(\Delta)_2Ti^0]$ and $[H_8N_4Ti^{IV}]$ does not seem to be reversible.

At this point, it is clear that porphyrinogen is able to satisfy the requirements of the metal at which it is coordinated, as far as electrons are concerned. With a metal that needs electrons, porphyrinogen assumes the structure with two cyclopropane units and it is able to donate up to four electrons, while with a metal that can be easily oxidized porphyrinogen accepts up to four electrons. The effect of any perturbation from the environment that will end with a variation in the oxidation state of the metal can be minimized by a rearrangement of the structure of the porphyrinogen. We conclude that the presence of the porphyrinogen coordinated to a metal has a buffering effect on the oxidation state of the metal. The only requirement is that electrons must be exchanged in couples; the removal of each couple corresponds to the formation of a cyclopropane unit on the porphyrinogen skeleton. This point does not exclude the possibility of a redox process involving only one electron; however, in this case the oxidation state of the metal must necessarily change, as shown in Scheme 3 (page 2920) for a metal which prefers a +2 oxidation state.

Conclusion

This study, at DFT level, has shown that transition metal Schiff base complexes and transition metal porphyrinogen complexes show similar, although complementary, behavior in redox processes. In transition metal Schiff base complexes C–C σ bonds are formed upon acquisition of pairs of electrons, while in transition metal porphyrinogen complexes, C–C σ bonds are formed upon loss of pairs of electrons. In both systems, the formation or the breaking of the C–C bonds avoids a variation in the oxidation state of the metal. These C–C bonds, therefore, act not only as electron reservoirs, but also as a buffer of the oxidation state of the metal. The lack of variation in the oxidation state of the metal is the first step towards the reversibility of the redox process. In the energetic balance of the whole redox cycle, however, it is also necessary to include the energetics of the reaction partner, and this point will be investigated in future work.

Acknowledgment

The present work has been carried out within the COST D9 Action.

[1] F. Franceschi, E. Solari, C. Floriani, M. Rosi, A. Chiesi-Villa, C. Rizzoli, *Chem. Eur. J.* **1999**, *5*, 708.
[2] E. Gallo, E. Solari, N. Re, C. Floriani, A. Chiesi-Villa, C. Rizzoli, *J. Am. Chem. Soc.* **1997**, *119*, 5144.
[3] E. Solari, C. Maltese, F. Franceschi, C. Floriani, A. Chiesi-Villa, C. Rizzoli, *J. Chem. Soc. Dalton Trans.* **1997**, 2903.
[4] S. De Angelis, E. Solari, E. Gallo, C. Floriani, A. Chiesi-Villa, C. Rizzoli, *Inorg. Chem.* **1996**, *35*, 5995.
[5] a) U. Piarulli, E. Solari, C. Floriani, A. Chiesi-Villa, C. Rizzoli, *J. Am. Chem. Soc.* **1996**, *118*, 3634; b) S. De Angelis, E. Solari, C. Floriani, A. Chiesi-Villa, C. Rizzoli, *J. Am. Chem. Soc.* **1994**, *116*, 5691; c) S. De Angelis, E. Solari, C. Floriani, A. Chiesi-Villa, C. Rizzoli, *J. Am. Chem. Soc.* **1994**, *116*, 5702.

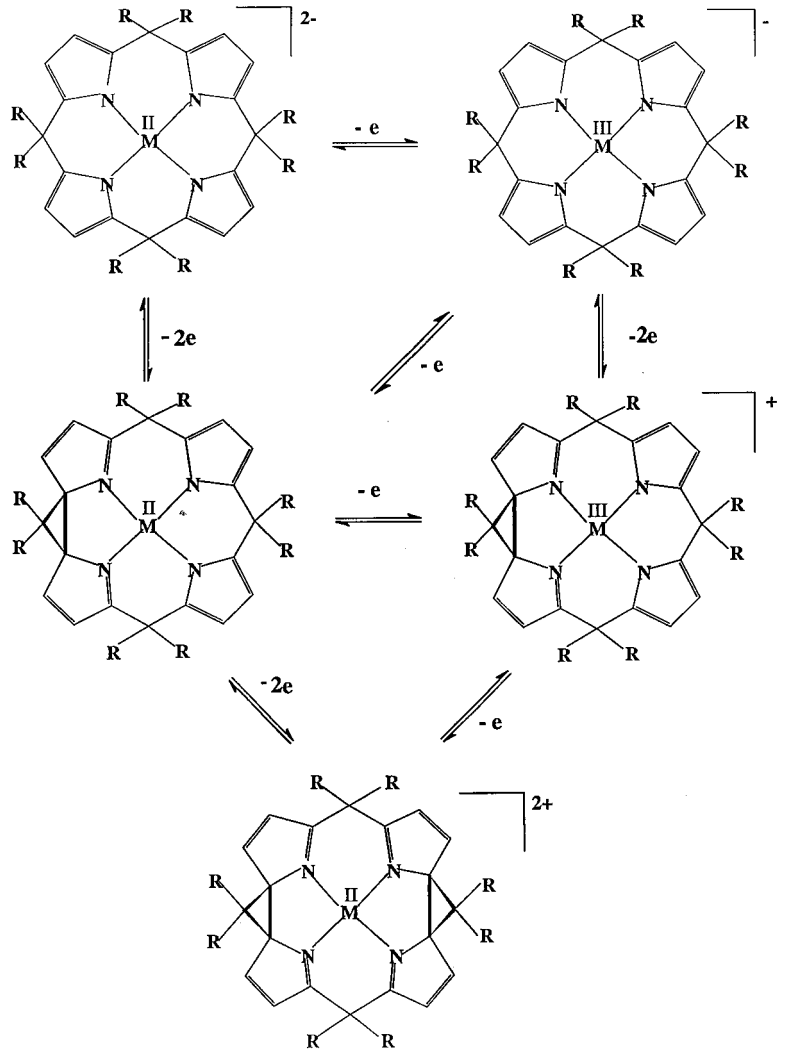

Scheme 3. Possible redox processes of a metal porphyrinogen complex.

[6] a) H. Fischer, H. Orth, *Die Chemie des Pyrrols*, Akademische Verlagsgesellschaft, Leipzig, Germany, **1934**, p. 20; b) M. Dennstedt, J. Zimmermann, *Chem. Ber.* **1887**, *20*, 850, 2449; M. Dennstedt, J. Zimmermann, *Chem. Ber.* **1888**, *21*, 1478; c) M. Dennstedt, *Chem. Ber.* **1890**, *23*, 1370; d) V. V. Chelintzev, B. V. Tronov, *J. Russ. Phys. Chem. Soc.* **1916**, *48*, 105, 127; e) Th. Sabalitschka, H. Haase, *Arch. Pharm.* **1928**, *226*, 484; f) P. Rothemund, C. L. Gage, *J. Am. Chem. Soc.* **1955**, *77*, 3340.

[7] a) C. Floriani, *Chem. Commun.* **1996**, 1257; b) C. Floriani, *Chimia* **1996**, *50*, 608.

[8] A. Ricca, C. W. Bauschlicher, *J. Phys. Chem.* **1994**, *98*, 12899.

[9] A. D. Becke, *Phys. Rev. A* **1988**, *38*, 3098.

[10] a) J. P. Perdew, *Phys. Rev. B* **1986**, *33*, 8822; b) J. P. Perdew, *Phys. Rev. B* **1986**, *34*, 7406.

[11] M. J. Frisch, G. W. Trucks, H. B. Schlegel, P. M. W. Gill, B. G. Johnson, M. A. Robb, J. R. Cheeseman, T. Keith, G. A. Peterson, J. A. Montgomery, K. Raghavachari, M. A. Al-Laham, V. G. Zakrzewski, J. V. Ortiz, J. B. Foresman, J. Cioslowski, B. B. Stefanov, A. Nanayakkara, M. Challacombe, C. Y. Peng, P. Y. Ayala, W. Chen, M. W. Wong, J. L. Andres, E. S. Replogle, R. Gomperts, R. L. Martin, D. J. Fox, J. S. Binkley, D. J. Defrees, J. Baker, J. J. P. Stewart, M. Head-Gordon, C. Gonzalez, J. A. Pople, *Gaussian 94*, Gaussian, Pittsburgh PA, **1995**.

[12] a) A. E. Reed, L. A. Curtiss, F. Weinhold, *Chem. Rev.* **1988**, *88*, 899, and references therein; b) J. E. Carpenter, F. Weinhold, *J. Mol. Struct. (Theochem)* **1988**, *169*, 41.

[13] E. D. Glendening, A. E. Reed, J. E. Carpenter, F. Weinhold, *NBO Version 3.1*.

[14] a) A. J. H. Wachters, *J. Chem. Phys.* **1970**, *52*, 1033; b) P. J. Hay, *J. Chem. Phys.* **1977**, *77*, 4377.

[15] M. J. Frisch, J. A. Pople, J. S. Binkley, *J. Chem. Phys.* **1984**, *80*, 3265, and references therein.

[16] T. Clark, J. Chandrasekhar, G. W. Spitznagel, P. von R. Schleyer, *J. Comput. Chem.* **1983**, *4*, 294.

[17] J. S. Binkley, J. A. Pople, W. J. Hehre, *J. Am. Chem. Soc.* **1980**, *102*, 939.

Received: December 28, 1998 [F1510]

  0947-6539/99/0510-2920 $ 17.50+.50/0